articles

An absorption feature in the spectrum of the pulsed hard X-ray flux from 4U0115+63

Wm. A. Wheaton, J. P. Doty, F. A. Primini, B. A. Cooke, C. A. Dobson, A. Goldman, M. Hecht, J. A. Hoffman*, S. K. Howe, A. Scheepmaker†, E. Y. Tsiang & W. H. G. Lewin

Department of Physics and Center for Space Research, Massachusetts Institute of Technology, Cambridge, Massachusetts 02139

J. L. Matteson, D. E. Gruber, W. A. Baity, R. Rothschild, F. K. Knight, P. Nolan & L. E. Peterson

Physics Department, University of California at San Diego, La Jolla, California 92093

A spectral feature, apparently an absorption line, has been observed at an energy of 20.1 ± 0.5 keV in the pulsed flux of 3.61 s X-ray pulsar 4U0115+63 using the UCSD/MIT instrument on HEAO 1. The line strength, expressed as equivalent width, is 3.1 ± 0.5 keV. Although essentially unresolved, the feature has a depth more than 60% of the continuum flux. If the feature arises by cyclotron resonance absorption near the magnetic poles of the neutron star, it implies a magnetic field of between ≈1.8 and ≈2.5 × 10^{12} G depending on the gravitational redshift (≲5–40%).

ALTHOUGH standard models (see ref. 1) of the pulsating binary X-ray sources as rotating, accreting magnetised neutron stars require magnetic fields B of the order of 10^{12}–10^{13} G, the discovery by Trümper *et al.*[2] of a strong pulsed 58 keV feature in 1976 and 1977 balloon observations of the spectrum of Her X-1 raised the important possibility of direct measurements of B. Trümper *et al.*[2] have argued that the feature they observed may result, as suggested earlier on theoretical grounds by Basko and Sunyaev[3], from cyclotron emission quantised in a field of ≈5.3 × 10^{12} G (uncorrected for redshift). The UCSD/MIT experiment on HEAO 1 confirmed the existence of this feature in the spectrum of Her X-1 on several occasions in 1978 (refs 4, 5).

The 1978 outburst[6,7] of 4U0115+63 led to discovery of its 3.61 s pulsations[6–8], accurate measurement of its position[9,10], and discovery of its binary nature[11], 24-d orbit[12], and 15th mag B-type optical counterpart[13], as well as the determination of X-ray spectra and pulse profiles from 0.9 to 40 keV[14,15]. Here we present details of the evidence for the 20 keV feature previously reported[16], but defer a complete discussion of the 12–180 keV spectral and temporal behaviour of the source. We caution that despite the attractiveness of the cyclotron interpretation of the feature, pending better understanding of the complex physics of radiation transfer in the magnetised, semi-relativistic atmosphere of an accreting neutron star, we cannot exclude the possibility that the observed phenomenon results from some quite different cause.

Observations

HEAO 1 pointed at 4U0115+63 (ref. 17) on 16 January 1978, when the source was near its peak brightness, for ≈3 h centred at ≈15.00 UT. Each of the two low energy detectors (LED1 and LED2) of the UCSD/MIT hard X-ray and low energy γ-ray experiment[18] had a ≈0.3 cm thick, actively shielded NaI 'phoswich' scintillation detector of area ≈100 cm^2 collimated to a 1.2° × 23° (FWHM) field-of-view by slat collimators with an energy resolution of ~6 keV (FWHM) at 20 keV. X-ray events in the 12–180 keV range are analysed in the 64-channel linear pulse height analyser (PHA) and transmitted event-by-event over a single telemetry channel shared among seven detectors. The mean residence time of events in the telemetry buffers determines the time resolution of about 0.05 s, binned here to 0.32 s. After elimination of Earth-blocked data and correction for electronic and telemetry dead times, each detector yielded about 6,000 s of useful data.

Fourier transforms and folds gave a best geocentric period of 3.61361 s during the observation, consistent with the SAS 3 ephemeris[12]. Figure 1 shows the data from LED2, folded modulo the pulse period and summed over the 12–66 keV interval in which we observe a significant pulsed flux. Comparison of this 'template' pulse shape with the data in individual PHA channels (Fig. 2) shows no strong variation of pulse profile with energy, but a marked reduction in pulse amplitude in the 19.3–24.8 keV band. In these circumstances it becomes possible to discuss the data in terms of a simple two-component model, in which we represent the observations as a sum of pulsed and steady fluxes. To determine the spectrum of each of these two components we fit the folded data in each PHA channel by the sum of two functions of the pulse phase—the first a constant, and the second given by the template. The smooth curves of Fig. 2 show the resulting fits. These smooth curves all have the same shape and phase alignment, which are those of the template. Only their amplitudes have been adjusted to fit the data. Because of minor differences in time and energy resolution and gain between the two detectors, we fit each independently, obtaining the spectra shown in Fig. 3.

* Permanent address: Astronaut Office, NASA Johnson Space Center, Houston, Texas 77058.

† Permanent address: Cosmic Ray Working Group, Leiden, The Netherlands.

0028/0836/79/460240—04$01.00

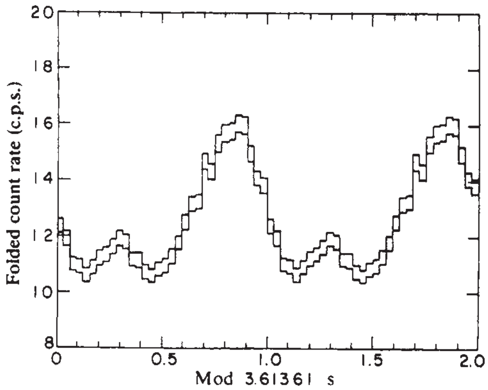

Fig. 1 Counting rates (12–66 keV) in low energy detector 2 (LED2) folded modulo the pulse period. LED1 shows a virtually identical profile. The upper and lower histograms show the data $\pm 1\sigma$, for two complete pulse periods. The data at any energy from 12 to 66 keV can be well represented by a sum of constant and a pulse of this shape. The plot includes a background count rate of 3.7 counts per second (c.p.s.). Phase 0 refers to JD 2443525.1134055.

The two lower sets of points (Fig. 3) show the pulsed spectrum in each detector, where we define the pulsed flux as the excess flux above the minimum of the fitted pulse profile, averaged over one 3.61 s cycle. Because the background is unpulsed, these spectra required no background subtraction, and their error bars reflect only counting statistics. This also allowed us to include data with the Earth's horizon in the field of view, which increases the useful exposure from the ≈3,800 s included in the total spectrum (and in our preliminary report[16]) to ≈6,000 s.

The large dip in the pulsed LED2 spectrum in PHA channels 9 and 10 corresponds to the low amplitude of pulsation noted in the 19.3–24.8 keV band of Fig. 2. The smaller dip in LED1 results partly from poorer resolution (since the feature is essentially unresolved—see below) in that detector, ≈33% (FWHM at 20 keV) as against ≈29% for LED2, and, we must conclude, partly from a statistical fluctuation. By a series of detector response calculations, detailed below, we have established that the combined probability (taking both detectors into account) that the observed feature could have arisen by a statistical fluctuation from a smooth continuum is very small ($\chi^2 = 50$ for $\nu = 7$ d.f.) but that adding a narrow absorption line to the model gives an improved χ^2 of 9.6 ($\nu = 5$) for the model of best fit. Because of the difference (in the depth the feature) between the two detectors, more complicated model photon spectra cannot be expected to improve χ^2 very much, so we accept the fit. For the model of best fit we obtained an absorption line energy $E_0 = 20.1 \pm 0.5$ keV and a line strength, expressed in terms of the equivalent width of continuum absorbed, of $\Delta E = 3.1 \pm 0.5$ keV. Independent fits to each detector separately yielded $\Delta E = 2.0 \pm 0.7$ keV for LED1 and $\Delta E = 4.1^{+1.1}_{-0.7}$ keV for LED2. Such an absorption line must have a depth exceeding 0.6 of the continuum level (95% confidence), which corresponds to a maximum actual width of about 5 keV (=3.1 keV/0.6). Systematic uncertainties, principally due to the idealised two-component analysis and to imperfections in the detector response models, may increase the absolute errors for E_0 and ΔE from the purely statistical errors quoted.

Experiments with different methods of analysis from those reported here, and with reasonable modifications of the detector response models, lead us to estimate the maximum likely increase in these errors to be less than a factor of two.

In these calculations we used response models for the two detectors based on pre-launch calibrations. We compared the expected counts for given input photon spectra with the actual data by a χ^2 test which treated the two detectors as a single experiment, summing χ^2 over the data from the five PHA channels nearest the feature in each detector. Systematic errors in the HEAO 1 attitude determination during the observation required independent normalisations for LED1 and LED2. Since we are concerned here only with the immediate vicinity of the feature, it was sufficient to use a simple form for the continuum, and we chose $dN/dE = A \exp(-E/E_\lambda)$. For the hypothesis of no feature we fitted for the continuum slope E_λ and the two normalisations, obtaining $\nu = 7$, and for the line hypothesis fits we added E_0 and ΔE, obtaining $\nu = 5$. We determined the single parameter, 1σ statistical errors in E_0 and ΔE, and the constraint on the line depth, using criteria discussed by Avni[19].

As the feature appears in the 3.61 s pulsed spectrum, it is very difficult to understand as an artefact of the instrument or analysis. It appears neither in the background nor in the unpulsed spectrum of 4U0115+63, nor in any other source spectra observed with the same instrument and analysed in the same way, whether pulsed (such as Her X-1, GX1+4, 4U0900−40 and 4U1626−67)[4,5,18] or total (Crab Nebula, Cyg X-1). We have divided the data into two halves, and the dip appears in each of them.

The two-component analysis which leads to the pulsed spectra of Fig. 3 has the important feature that, in the language of signal processing, it filters the data with the expected signal shape (the template), which yields optimal sensitivity. However, if there is a strong variation with energy of pulse profile or phasing this

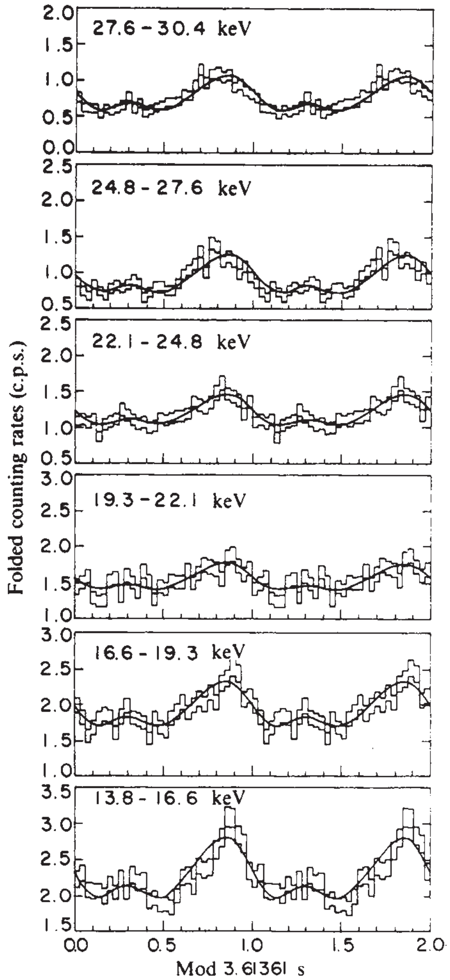

Fig. 2 Folded counting rates from LED2 in PHA channels 7–12, displayed similarly to Fig. 1, all to the same scale. The 19.3–24.8 keV channels (PHA 9 and 10) are noticeably less strongly pulsed than adjacent channels, possibly due to cyclotron resonance absorption. The continuous curves show fitted pulse profiles derived as described in the text, only smoothed for clarity by omission of all but the first three Fourier frequencies. Background rates for PHA channels 7 to 12 of 0.48, 0.37, 0.30, 0.26, 0.23 and 0.24 (c.p.s.), respectively, are included.

analysis could introduce spurious features. Data taken simultaneously by the Goddard Space Flight Center experiment on HEAO 1 show rapid changes in overall pulse shape with energy below about 10 keV (ref. 21) but examination of the data above 13 keV and the fits in Fig. 2 shows only small changes in pulse profile, which do not change the general shape or phase of the pulse, even in the channels with the dip, and do not account for the reduction in pulse amplitude there. A χ^2 test of the data in each PHA channel against the hypothesis of no pulsation gave $\chi^2 = 90$ (for 31 d.f.) in the channel with the dip, but $\chi^2 = 150$–190 at both higher and lower energies, which establishes the reality of the feature independent of any assumptions about pulse shape. Pravdo *et al.*[22] pointed out that incautious subtraction of physically different 'on-pulse' and 'off-pulse' spectra could produce an apparent absorption feature with no underlying physical significance. While one can never rigorously exclude such an explanation, the deep and narrow feature observed make it artificial in this case. We observe a pulse that varies strongly in amplitude but very little in shape as a function of energy. For such behaviour the picture of independent emission spectra with pulse phase offers no natural interpretation.

The two upper sets of data in Fig. 3 show the total (pulsed plus unpulsed) spectrum in each detector. In the analysis of these total spectra we used only data in which the Earth lay completely outside the collimator field of view in order to avoid large systematic background variations. We estimated the background from ≈4,000 s of sky exposure in each detector obtained in eight roughly equal intervals from the two orbits of scanning data adjacent to the observation; the errors shown for the total spectra include the effects of systematic variations in the background as estimated from the scatter among these eight intervals. Figure 4 shows the photon spectrum for LED2 corresponding to the total count spectrum of Fig. 3*b*, derived by dividing by detector efficiencies determined from the instrument response to the Crab Nebula. The spectrum is close to a power law with number spectral index ≈3.9 or to ≈10^8 K thermal bremsstrahlung. A correction of 0.85 for the collimator transmission averaged over small aspect variations during the point was applied.

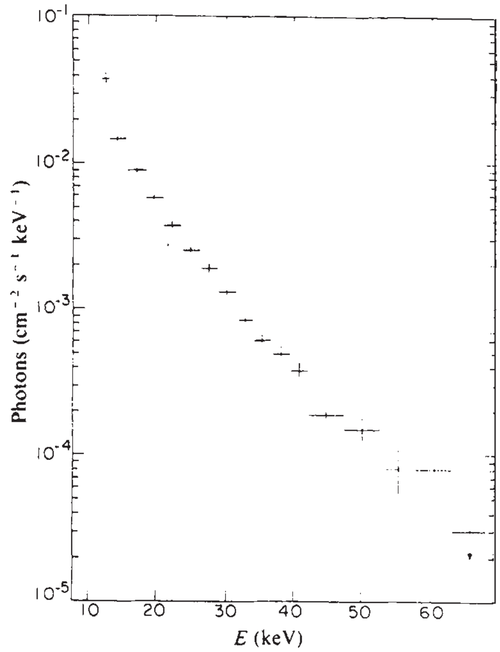

Fig. 4 Photon spectrum of the total flux (pulsed plus unpulsed), using the data from Fig. 3*b*, and based on a calibration using the Crab Nebula.

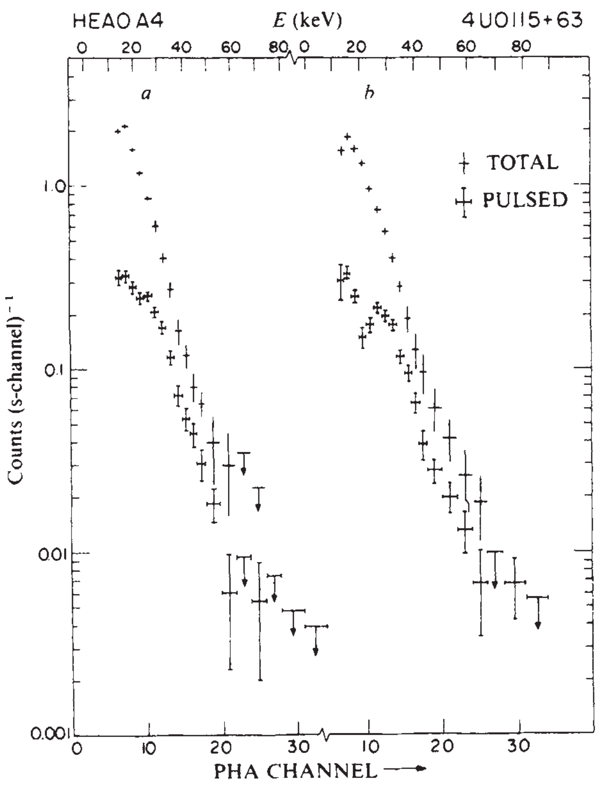

Fig. 3 Pulse height spectra of the total (upper) and pulsed (lower) counts in: *a*, LED1; and *b*, LED2. The 20 keV feature shows most clearly in LED2 in PHA channel 9. If it results from cyclotron resonance absorption, it corresponds to a surface magnetic field B of ~1.8–2.5×10^{12} G, (depending on the gravitational redshift), probably near the poles of the neutron star.

Discussion

Our results are consistent with all the other data known to us. However, the UCSD/MIT observation obtained about an order of magnitude more counts in the 20 keV range than any other instrument of comparable energy resolution. Hence no detailed confirmation of the 20 keV feature seems likely until further observations can be obtained.

Figure 3 shows that the pulse fraction, defined here as the ratio (pulsed flux)/(total flux), decreases from ≈50% at 60 keV to ≈17% at 15 keV. Johnston *et al.*[14] have found that it continues to decline to below 2.5 keV. Because the pulsed spectrum is harder than the total spectrum, the spectrum must harden near the peak of the pulse, behaviour generally similar to that seen from 0.9 to 18 keV by others[14,15]. However, the main peak observed below about 10 keV occurs at a different phase, about 0.5 instead of our 0.85.

Note that we use the term 'absorption' to include 'cyclotron resonance scattering'. The concavity of the total flux (Fig. 4) near 20 keV is sufficient to accomodate either absorption, which would entirely remove photons, or scattering, which could merely redistributate them in direction and thus pulse phase. However, as scattered photons could be beamed in directions never seen by Earth-bound observers, the two are essentially indistinguishable observationally.

The results for Her X-1 due to Trümper *et al.*[2] can be interpreted as absorption at energies below ≈42 keV as well as emission at ~58 keV. The data presented here, because of the deep and narrow feature, favour absorption/scattering as the correct interpretation for 4U0115+63 but cannot rule out an emission line explanation, in which the broad (about twice the instrument energy resolution) hump around 28 keV in the pulsed spectrum results from an emission blend seen over a steeply falling continuum. If due to cyclotron emission, our data would indicate a correspondingly higher and less uniform magnetic field. As we expect a cutoff in cyclotron emission corresponding to the maximum surface field near the magnetic poles, the observed extension of the pulsed flux above the feature suggests an additional hard component of the continuum. No full theoretical treatment predicting the relative likelihood of cyclotron emission or absorption/scattering has yet appeared, though each has been briefly considered in the literature[3,23,24]. Dimensional estimates tend to support scattering/absorption over emission (F. Lamb, personal communication). Clear evidence for higher (or lower) harmonics could settle this question, but it does not appear in these data.

Assuming that the 20 keV feature arises near the surface of the neutron star, a gravitational redshift of $\leq$5–40% (ref. 25) gives 20–28 keV as the surface energy corresponding to a 20 keV line. If, following Trümper *et al.*[2] we interpret this as due to cyclotron absorption from the ground state ($j=0$, $s=-1$) to the first excited state ($j=1$, $s=-1$) or ($j=0$, $s=+1$) and assume negligible change in the electron momentum parallel to the magnetic field B, we obtain $B \approx (1.8 \text{ to } 2.5)\times 10^{12}$ G, probably near the base of the accretion column near the magnetic pole. The narrowness of the line implies it must arise in a region of fairly uniform field, since $\Delta B/B \approx \Delta E/E \leq 0.25$. Because the radial extent Δr of the absorbing region must satisfy $\Delta r/r \leq \frac{1}{3}(\Delta B/B)$ (ref. 2), if $r \approx 10$ km, then Δr must be <1 km. Since redistribution of photons in energy would tend to fill in a narrow absorption line, its width and strength limit the amount of reprocessing matter that can lie along the line of sight. Thus, this source does not seem to be observed through a cold magnetospheric shell of the type proposed for Her X-1 (refs 26, 27), as discussed in detail by Weaver[28].

As we have already constrained the height of the emission region to <1 km, any future improvements in resolution will begin to show whether it is more like the size of the accretion hot spot ($\approx$1 km) or the atmospheric scale height ($\approx$1 m). Thermal motions along the magnetic field line should also contribute to the linewidth. Since this effect depends on the cosine of the angle between the field and the line of sight, observation of the broadening as a function of pulse phase could eventually give both the temperature of the absorbing electrons and the geometry of the system.

We thank members of the HEAO project and the people in the HEAO Operations Control Center for their work on making the pointed observation successful. We also thank L. A. Rose and S. Pravdo for comments and for results from the GSFC experiment prior to publication, and J. Trümper, L. Cominsky, J. McClintock, B. Rossi and J. van Paradijs for helpful comments. This work was supported by NASA contracts 8-27974 and 8-27975.

Received 10 May; accepted 31 August 1979.

1. Lamb, F. K. *Ann. N.Y. Acad. Sci.* **302,** 482 (1977).
2. Trümper, J., Pietsch, W., Reppin, C. & Voges, W. *Astrophys. J. Lett.* **219,** L105–L110 (1978); *Ann. N.Y. Acad. Sci.* **302,** 538 (1977).
3. Basko, M. M. & Sunyaev, R. A. *Astr. Astrophys.* **42,** 311–321 (1975).
4. Matteson, J. L., Gruber, D. E. & Hoffman, J. A. in *Gama Ray Spectroscopy in Astrophysics* **386,** (NASA TM 79619, 1978).
5. Gruber, D. E. *et al. Bull Am. astr. Soc.* **10,** 506 (1978).
6. Holt, S. S. & Kaluzienski, L. J. *IAU Circ.* No, 3161 (1978).
7. Clark, G. & Cominsky, L. *IAU Circ.* No. 3161 (1978).
8. Cominsky, L., Clark, G. W., Li, F., Mayer, W. & Rappaport, S. *Nature* **273,** 367–369 (1978).
9. Cominsky, L., Li, F., Bradt, H., Clark, G. W., & Rappaport, S. *IAU Circ.* No. 3163 (1978).
10. Johnston, M. *et al. IAU Circ.* No. 3163 (1978).
11. Rappaport, S., Clark, G., Cominsky, L., & Li, F. *IAU Circ.* No. 3171 (1978).
12. Rappaport, S., Clark, G. W., Cominsky, L., Joss, P. C. & Li, F. *Astrophy. J. Lett.* **224,** L1–L4 (1978).
13. Johns, M., Koshi, A., Canizares, C. & McClintock, J. *IAU Circ.* No. 3171 (1978).
14. Johnston, M. *et al. Astrophys. J. Lett.* **223,** L71–L73 (1978).
15. Rose, L. A. *et al.* preprint (1978).
16. Wheaton, W. A. & HEAO A4 Group, *IAU Circ.* No. 3238 (1978).
17. Forman, W., Jones, C. & Tananbaum, H. *Astrophys. J. Lett.* **206,** L29–L35 (1976).
18. Matteson, J. L. *Proc. AIAA 16th Aerospace Sci. Meet.*, Huntsville, Alabama, pap. 78–35, (1978).
19. Avni, Y. *Astrophys. J.* **210,** 642–646 (1976).
20. Doty, J. *et al. Bull. Am. astr. Soc.* **10,** 507 (1978).
21. Pravdo, S. H. *et al. Bull. Am. astr. Soc.* **10,** 446 (1978).
22. Pravdo, S. H. *et al.* preprint (1978).
23. Ginedin, Y. N. & Sunyaev, R. A. *Astr. Astrophys.* **36,** 379–394 (1974).
24. Elsner, R. F. & Lamb, F. K. *Nature* **262,** 356–360 (1976).
25. Arnett, W. D. & Bowers, R. L. *Astrophys. J. Suppl.* **33,** 415 (1977).
26. McCray, R. & Lamb, F. K. *Astrophys. J. Lett.* **204,** L115–L118 (1976).
27. Basko, M. M. & Sunyaev, R. A. *Mon. Not. R. astr. Soc.* **175,** 395 (1976).
28. Weaver, R. P. *Nature* **274,** 571–572 (1978).

Plasma acceleration at the Earth's magnetopause: evidence for reconnection

G. Paschmann, B. U. Ö. Sonnerup*, I. Papamastorakis, N. Sckopke & G. Haerendel

Max-Planck-Institut für Physik und Astrophysik, Institut für extraterrestrische Physik, 8046 Garching, FRG

S. J. Bame, J. R. Asbridge & J. T. Gosling

University of California, Los Alamos Scientific Laboratory, Los Alamos, New Mexico 87545

C. T. Russell & R. C. Elphic

University of California at Los Angeles, Institute of Geophysics and Planetary Physics Los Angeles, California 90024

A characteristic of magnetic field reconnection is the acceleration of plasma as it flows across a rotational discontinuity. At the Earth's magnetopause this effect has only been observed recently during a few magnetopause crossings by the ISEE satellites. For one example analysed in detail the results show good agreement with theoretical predictions.

MAGNETIC reconnection or merging is thought to have a fundamental role in the conversion of energy stored in magnetic fields, and may occur in many cosmic situations. The concept of reconnection was introduced into magnetospheric physics by Dungey[1] who proposed that reconnection should be operative at the dayside boundary of the Earth's magnetic field, the magnetopause, as well as in the geomagnetic tail. A detailed description of the process was first provided by Petschek and coworkers[2,3] who demonstrated that reconnection may occur at substantial rates and that it leads to high-speed plasma jetting away from the reconnection site. Jets of plasma possibly associated with reconnection have been observed in the tail[4,5] but never at the magnetopause. This negative result has added to the controversy over the nature and efficiency of the reconnection process, despite substantial indirect evidence for its occurrence[6]. Recent measurements from the dual-satellite International Sun–Earth–Explorer Mission[7] (ISEE) have now shown the occasional presence of high-speed plasma at the magnetopause. We report here on one of these cases in which the observations agree in considerable detail with theoretical predictions.

The basic reconnection configuration for the magnetopause[3,8] is illustrated in Fig. 1. In this model, the magnetopause is a standing Alfvén wave emerging from the X-shaped centre of the

* Permanent address: Dartmouth College, Radiophysics Laboratory, Hanover, New Hampshire 03755.

0028/0836/79/460243—04$01.00